# Influence of shape and size on GaN/InGaN $\mu$LED light emission: a competition between sidewall defects and light extraction efficiency

Palmerina Gonzalez Izquierdo, Névine Rochat, Davide Zoccarato, Fabian Rol, Julia Simon, Patrick Le Maitre, Matthew Charles, Matthieu Lafossas, Simona Torrengo, Lukasz Borowik

# Influence of shape and size on GaN/InGaN μLED light emission: a competition between sidewall defects and light extraction efficiency

*Palmerina González-Izquierdo*, Névine Rochat, Davide Zoccarato, Fabian Rol, Julia Simon, Patrick Le Maitre, Marion Volpert, Matthew Charles, Matthieu Lafossas, Simona Torrengo and Łukasz Borowik**

Univ. Grenoble Alpes, CEA, Leti, F-38000 Grenoble, France

**KEYWORDS:** micro light-emitting diodes, InGaN, sidewall defects, quantum efficiency, light extraction efficiency, shape, size, geometry.

ABSTRACT: Micro light-emitting diodes (μLEDs) are expected to revolutionize the display technology due to their advantages over the current LCD and OLED technology and the possibility to use them in micro displays, visible light communications and optogenetics. One of the main challenges of this emergent technology is the efficiency drop with the reduction of LED size due to sidewall defects. In this paper, we study the size and shape dependence of the external quantum efficiency (EQE) by cathodoluminescence measurements at room temperature and 10 K. Our results show that, for small μLEDs (between 2.5 and 10 μm width), there is an optimal intermediate LED size for which the light emission is maximized, which we attribute to a competition between the light extraction efficiency (which decreases with LED size) and the internal quantum efficiency (which increases with LED size). In contrast to most prior studies that typically examine either IQE or LEE with respect to size for larger LEDs, our work stands out by examining the interplay between IQE and LEE for μLEDs below 10 μm. These results are of high relevance for the design of μLED arrays and show the need for understanding the evolution of light extraction efficiency and sidewall non-radiative recombination with LED geometry and size.

**Introduction:**

Light emitting diodes (LEDs) have become the most efficient artificial light source[1] since the development of the blue LED in 1988,[2] with common chip sizes of (300 × 300) μm$^2$ or larger. Nowadays, a significant interest is directed towards the miniaturization of LEDs below (100 × 100) μm$^2$ down to 1 μm$^2$ because of their many possible applications: improvement comparted to current LCD (Liquid Crystal Display) and OLED (Organic LED) display technologies, augmented and virtual reality, visible light communication (VLC) or optogenetics.[3–7] However, one of the main challenges of this emerging technology is the decrease of device efficiency with the reduction of LED size due to the non-radiative recombination through defect energy levels introduced during the etching process.[8,9] Although many studies have been carried out to study LED performance dependence with size,[10–13] most of the literature focuses on relatively large LEDs, from (500 × 500) μm$^2$ down to (10 × 10) μm$^2$. The majority of papers investigate the size dependence of the external quantum efficiency (EQE), which depends on two factors: the internal quantum efficiency (IQE), affected by the radiative and non-radiative recombination, and the light extraction efficiency (LEE) from the device. Two approaches[14] are often employed in order to increase the efficiency of LEDs: increasing IQE through the reduction of sidewall defects using post-etching passivation[15–19] and/or improving light extraction by using a favorable LED design.[20–23] However, the interplay between IQE and LEE as a function of LED size is difficult to decorrelate.[20,24] In this paper, we study the dependence of light emission of square and circular-shaped LED mesa structures of various sizes (2.5, 5, 7.5 and 10 μm) through cathodoluminescence, which enables us to map the light emission with nanometric resolution. By performing measurements on the same mesas at room temperature (RT) and 10 K (where the defect-related energy states are inactive), we were able to separate the LEE and IQE contributions to the EQE and find their respective dependence with size and geometry, which paves the way towards the efficient miniaturization of LEDs.

**Experimental methods:**

InGaN based LED structures were grown on 200 mm diameter Si(111) substrates by metalorganic vapor phase epitaxy (MOVPE) using an AIXTRON Crius-R200 growth tool. The structure

consists of an AlN nucleation layer, AlGaN buffer layers, and 600 nm of non-intentionally doped GaN. This was followed by 1 µm of n-type GaN, doped with silicon at $5\times10^{18}$ $cm^{-3}$, an active region consisting of five InGaN multiple quantum wells (MQW) of 2.5 nm separated by 8 nm GaN barriers, a 20 nm thick $Al_{0.15}Ga_{0.85}N$ electron blocking layer (EBL) and finally 200 nm p-type Mg-doped GaN with a 20 nm p+ highly doped layer. A transparent p-contact is fabricated by ITO (Indium tin oxide) deposition. The epi-LED stack is then partially etched using chlorine based ICP (Inductively Coupled Plasma) process. In an additional step suitable for cathodoluminescence (CL) measurement, the remaining hard-mask and ITO layer on top of the LED pixel are removed by wet process (HF + HCl 37%).

Cathodoluminescence measurements were performed using an Attolight CL microscope. The sample was excited by an electron beam with an acceleration voltage of 10 keV and a beam current of 12 nA. This primary beam acceleration voltage was chosen in order to probe the multi-quantum well region of the mesa structures (Monte Carlo simulation with Casino[25] software). The luminescence was collected through an integrated light microscope (Numerical Aperture: 0.72) embedded within the electron objective lens, giving an optical collection of 200 µm around the excited area. We assume negligible crosstalk in our GaN-on-Si epi-LEDs. Unlike GaN on sapphire, where light propagates through the sapphire substrate, in our case, the Si substrate absorbs the light, effectively suppressing crosstalk.[26] By scanning the sample, the optical spectra of each pixel of the secondary electrons (SE) image are recorded on a CCD camera through a dispersive spectrometer (focal length: 320 mm, grating: 150 grooves/mm). Four circular and four square mesa structures of different sizes were measured at room temperature (5 and 10 ms/px, respectively) and 10 K (1 ms/px). Intensities are normalized to the highest value for each mesa shape to avoid instrumental variability between the two geometry series and highlight the impact of mesa size. The CL intensity maps obtained at both temperatures were aligned with reference to their SE images using a Python routine developed at CEA.

**Results and discussion:**

Fig. 1 shows the integrated intensity maps over the MQW emission peak (from 390 to 520 nm) at room temperature for four square and circular epi-LED mesa structures of different sizes. Fig. 2 shows the integrated intensity profiles, averaged over the area marked as red rectangles in Fig. 1 in the vertical direction, and the maximum and mean intensity (over the central area of the

rectangle) with its standard deviation. Both series of circular and square mesas have the same widths (approx. 2.5, 5, 7.5 and 10 µm) in order to be able compare their behavior, as the Shockley-Read-Hall (SRH) recombination depends on the perimeter-to-surface ratio.[27] As expected, we observe a reduction of the CL signal near the edge of the mesas due to non-radiative recombination through sidewall defect energy levels. For the largest mesas, the maximum CL intensity is reached between 3 and 3.5 µm from the edge, a distance which is much greater than the minority carrier diffusion length in GaN (typically ranging from 100 nm to 1 µm)[28–30] or InGaN.[31] However, it is consistent with the values reported for high quality InGaN QWs[32] and AlGaN.[33] Indeed, similar CL studies carried out on mesa structures without an AlGaN EBL showed that the detrimental effect in the light emission due to the edges occurred over a smaller distance (around 800 nm).[34] Therefore, for the two smaller mesas, the whole volume is affected by non-radiative recombination through sidewall defects. We should note that the measured CL intensity values for the circular mesa with a size of 7.5 µm have a broad distribution; the observed intensity fluctuations in Figs. 1 and 2.a, along with the higher standard deviation presented in Fig. 2.b, suggest caution in interpreting and drawing firm conclusions from this specific dataset. These fluctuations could potentially arise from various factors, including dislocations[35,36] point defects[37] and/or lateral epitaxial inhomogeneities. Both mesa geometries show the same trend: as expected, the emitted light increases with the size of the mesa, ranging from 2.5 to 7.5 µm. This rise can be attributed to the diminishing detrimental effect of sidewall defects with the decrease of perimeter-to-surface ratio. However, a sudden intensity drop occurs for the largest mesa, as clearly seen in Fig. 2.b. A favorable EQE peak for green µLEDs with diameter below 10 µm has been previously reported,[38] but this phenomenon still lacks interpretation.

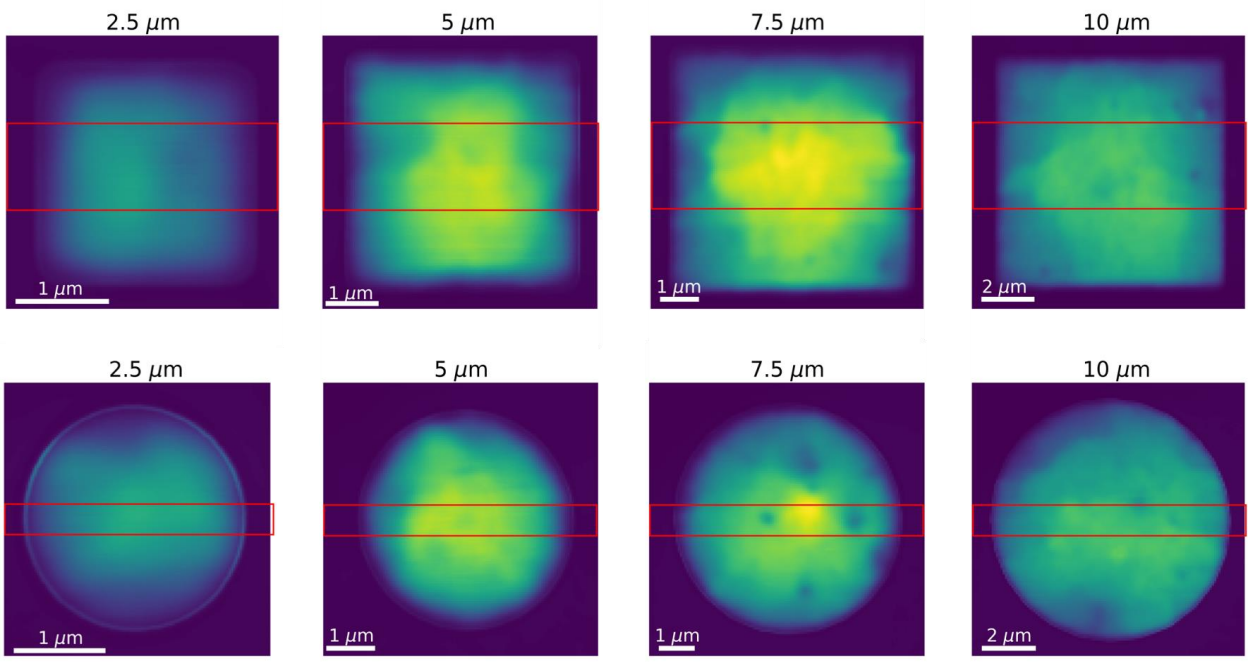


**Figure 1.** Integrated MQW cathodoluminescence intensity maps at room temperature for four square and circular mesas with different widths (2.5, 5, 7.5 and 10 μm). Mesas of the same geometry are presented using the same color scale that covers the intensity range of the mesa showing the highest intensity value within the series.

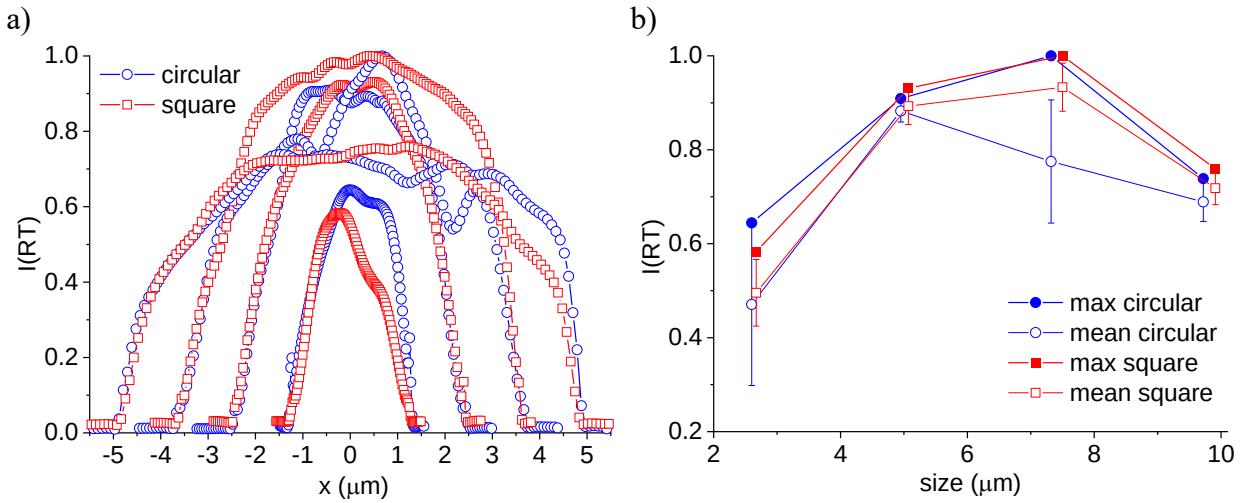


**Figure 2.** a) Integrated MQW cathodoluminescence profile at room temperature, normalized to the highest value for each shape, and averaged in the vertical direction over the area marked as red rectangles in Fig. 1, for four different sized square/circular mesas. b) Maximum (filled markers) and mean intensity over the central area of the mesas (empty markers) obtained from graph a.

This striking result can be understood by separating the two factors contributing to the CL signal, which are directly related to the EQE, which can be expressed as:

$$EQE = IQE \cdot LEE$$

In order to examine the LEE component, we performed the same measurements at 10 K to reduce the non-radiative recombination. When approaching 0 K, SRH recombination is avoided and the IQE tends to 1. Therefore, the light emission measured at low temperature (LT) is governed by the LEE. The integrated intensity maps over the MQW emission peak, the averaged intensity profiles and the mean intensities (over the central area of the mesas) and maxima at 10 K are shown in Figs. 3, 4.a, and 4.b, respectively. The first observation is that, aside from occasional variations, the CL signal maintains a uniform distribution across the mesa (see Figs. 3, 4.a), contrary to the measurements at RT, in which there was a considerable signal reduction near the edge. This confirms that the non-radiative recombination through defect energy states on the mesa edges is practically nullified at low temperature. However, the intensity fluctuations over the mesa remain observable at LT. This could be attributed to the fact that we are not operating at 0 K, causing these defects to remain partially unfrozen, or to non-radiative recombination through tunneling-assisted transitions.[39] Alternatively, for dislocations, the variations in intensity might relate to exciton dissociation prompted by the surface piezoelectric field. This could also explain why the fluctuations are shorter-range compared to sidewall defects, as the former are not related to the carrier diffusion length.[40] For square mesas, the two smallest mesas have a similar maximum light intensity (better appreciated in Fig. 4), and the larger ones show a linear decrease with the epi-LED structure size. This result is in agreement with reported simulations of LEE comparing square and circular mesa geometries, predicting a plateau for small square LEDs.[24] However, the circular mesas exhibit different behavior, with a CL signal reduction that occurs between the 2.5 μm and 5 μm mesas, before stabilizing between the 7.5 μm and 10 μm size mesas, also in agreement with LEE simulations for circular LEDs.[15,24]

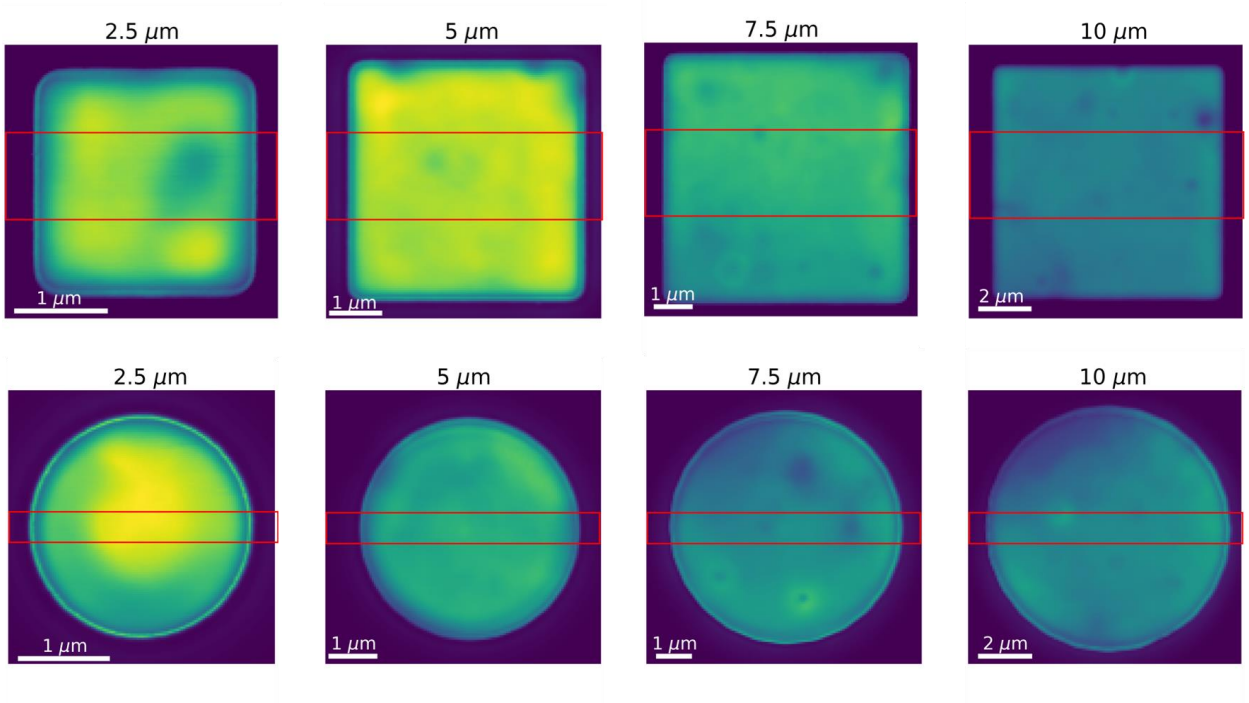


**Figure 3** Integrated MQW cathodoluminescence intensity maps at 10 K for four square and circular mesas with different widths (2.5, 5, 7.5 and 10 μm). Mesas of the same geometry are presented using the same color scale that covers the intensity range of the mesa showing the highest intensity value within the series.

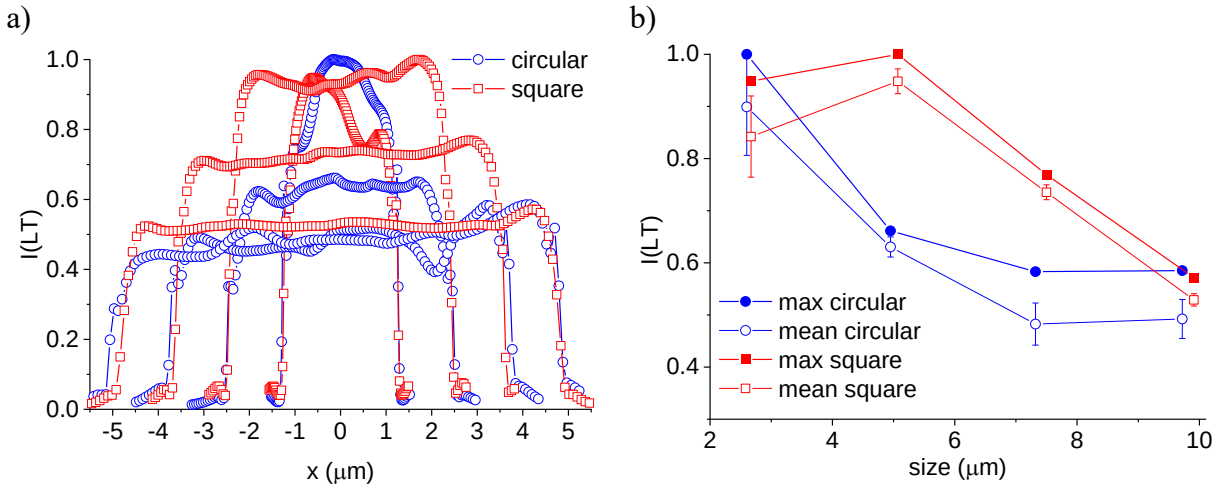


**Figure 4.** a) Integrated MQW cathodoluminescence profile at 10 K, normalized to the highest value for each shape, and averaged in the vertical direction over the area marked as red rectangles in Fig. 3, for four different sized square/circular mesas. b) Maximum (filled markers) and mean intensity over the central area of the mesas (empty markers) obtained from graph a.

Finally, we obtained the ratio of the CL intensity at RT and 10 K, which is governed by the IQE (considering that the IQE at LT tends to 1 and assuming that LEE does not depend on temperature). The resulting maps and profiles of this ratio are shown in Figs. 5 and 6, respectively. For both geometries, the I(RT)/I(LT) ratio increases from 2.5 up to 7.5 µm, corresponding to the mesas where the entire volume or nearly the entire volume is affected by the SRH recombination through sidewall defects due to extensive carrier diffusion (around 3.5 µm).[41] In the case of the square mesas, there is a subsequent attenuation of this increase as the relative importance of SRH recombination diminishes with the surface-to-perimeter ratio. A sudden decrease in I(RT)/I(LT) is observed for the 10 µm circular mesa. However, as stated previously, the CL intensity values measured for the 7.5 µm size at RT exhibit a broad distribution, as seen in the mean and standard deviation presented in Fig. 4.b. Consequently, caution must be exercised in drawing conclusions regarding whether this decrease represents a genuine decline or a dampening effect similar to that observed in the case of square mesas.

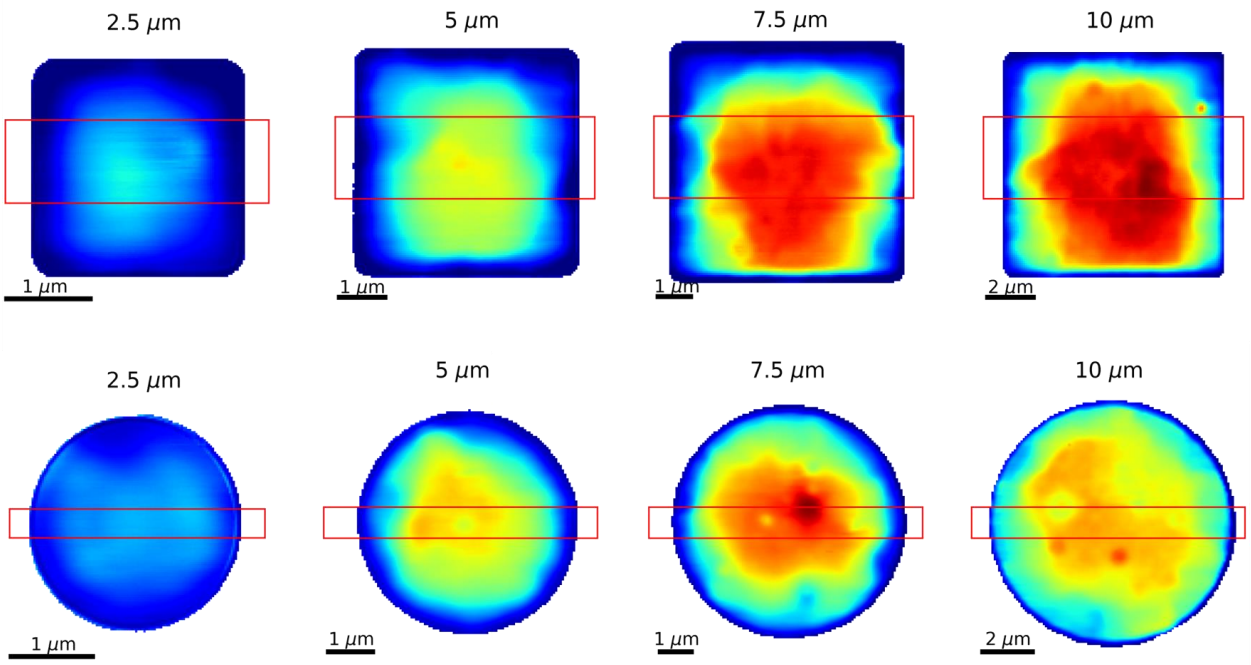


**Figure 5.** MQW I(RT)/I(LT) maps (color scale normalized to the maximum value of each geometry series) for four square and circular mesas with different widths (2.5, 5, 7.5 and 10 µm). Mesas of the same geometry are presented using the same color scale that covers the value range of the mesa showing the highest value within the series.

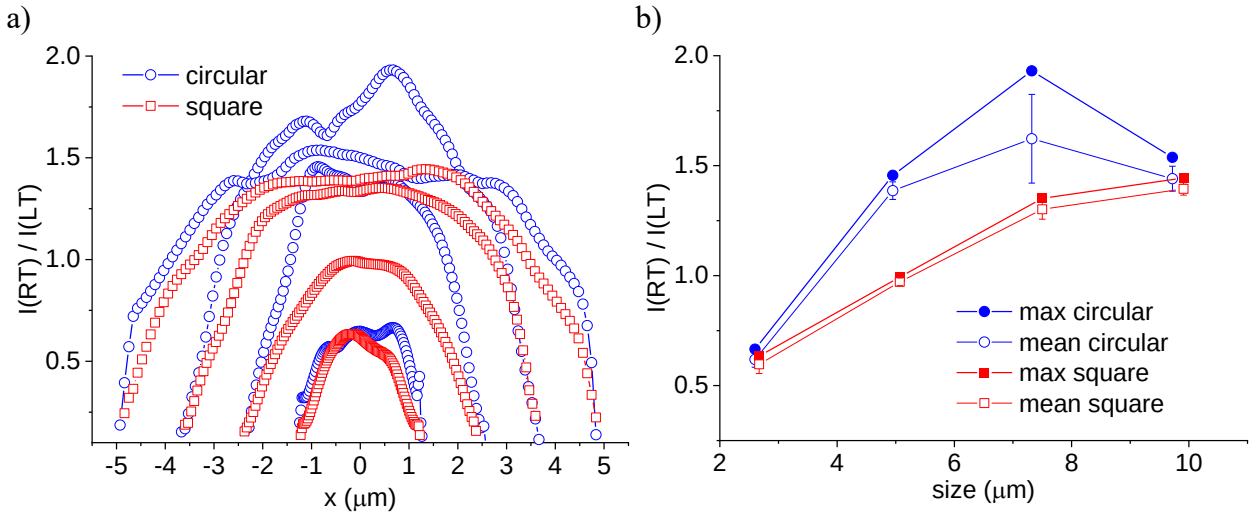


**Figure 6.** a) MQW I(RT)/I(LT) profile from normalized intensities, averaged in the vertical direction over the area marked as red rectangles in Fig. 5, for four different sized square/circular mesas. b) Maximum (filled markers) and mean value over the central area of the mesas (empty markers) obtained from graph a.

These analyses show that the optimal light emission for the intermediate-sized 7.5 μm mesa structures at RT can be explained by an interplay between the LEE and the IQE for both geometries: the LEE decreases with the size of the mesa, while the IQE is governed by non-radiative recombination through sidewall defects, which affects the mesas with higher perimeter-to-surface ratio the most. It is worth noting that the reported results, obtained at a specific charge carrier density (excitation at 10 kV), are subject to the dependency of the maximum EQE on this quantity as per the ABC model.

**Conclusion:**

In this paper, we studied the dependence of light emission in micro epi-LED mesa structures with different widths (2.5, 5, 7.5 and 10 μm) and geometries (square and circular). The results show an optimal intermediate mesa size, with a diameter lower than 10 μm, as a consequence of a competition between the light extraction efficiency (which decreases with size and shows a different trend for square and circular geometries) and non-radiative recombination on the mesa edges (which is greater for LEDs whose distance from the center to the edge is shorter or near the

minority carrier diffusion length). These findings illustrate the importance of understanding the relationship of IQE and LEE with respect to LED size and geometry in the path towards μLED array design.

## AUTHOR INFORMATION


### Corresponding Author

*Łukasz Borowik – Université de Grenoble Alpes, CEA, Leti, F38000 Grenoble, France

Email: lukasz.borowik@cea.fr

*Palmerina González Izquierdo – Université de Grenoble Alpes, CEA, Leti, F38000 Grenoble, France

Email: palmerina.gonzalezizquierdo@cea.fr


### Author Contributions

N.R. and D.Z. measured cathodoluminescence data. M.C., M.L. and S.T.grew the sample. F.R., J.S., P.LM. and M.V. did the sample processing, L.B., N.R. and P.G.I. conceptualized the project. P.G.I. analyzed the data and wrote the paper, with input from all other authors. All authors have given approval to the final version of the manuscript.


### Funding Sources

This work, carried out on the Platform for Nanocharacterisation (PFNC), was supported by the "Recherches Technologiques de Base" program and Carnot funding of the French National Research Agency (ANR).

## ACKNOWLEDGMENTS

We thank the "Recherches Technologiques de Base" program and Carnot funding of the French National Research Agency (ANR).


## REFERENCES


(1) Cho, J.; Park, J. H.; Kim, J. K.; Schubert, E. F. White Light-Emitting Diodes: History, Progress, and Future. *Laser and Photonics Reviews*. 2017. https://doi.org/10.1002/lpor.201600147.

(2) AKASAKI, I. High Efficiency Blue LED Utilizing GaN Film with AIN Buffer Layer by MOVPE. *Inst. Phys. Coference Ser.* **1988**, *91*, 633.
(3) Parbrook, P. J.; Corbett, B.; Han, J.; Seong, T.-Y.; Amano, H. Micro-Light Emitting Diode: From Chips to Applications. *Laser Photonics Rev.* **2021**, *15* (5), 2000133. https://doi.org/10.1002/lpor.202000133.
(4) Lin, J. Y.; Jiang, H. X. Development of MicroLED. *Appl. Phys. Lett.* **2020**, *116* (10), 100502. https://doi.org/10.1063/1.5145201.
(5) Templier, F. GaN-Based Emissive Microdisplays: A Very Promising Technology for Compact, Ultra-High Brightness Display Systems. *J. Soc. Inf. Disp.* **2016**, *24* (11), 669–675. https://doi.org/10.1002/jsid.516.
(6) Wang, Z.; Shan, X.; Cui, X.; Tian, P. Characteristics and Techniques of GaN-Based Micro-LEDs for Application in next-Generation Display. *J. Semicond.* **2020**, *41* (4), 041606. https://doi.org/10.1088/1674-4926/41/4/041606.
(7) Wei, Z.; Wang, L.; Li, Z.; Chen, C.-J.; Wu, M.-C.; Wang, L.; Fu, H. Y. Micro-LEDs Illuminate Visible Light Communication. *IEEE Commun. Mag.* **2023**, *61* (4), 108–114. https://doi.org/10.1109/MCOM.002.2200109.
(8) Boussadi, Y.; Rochat, N.; Barnes, J.-P.; Bakir, B. B.; Ferrandis, P.; Masenelli, B.; Licitra, C. Investigation of Sidewall Damage Induced by Reactive Ion Etching on AlGaInP MESA for Micro-LED Application. *J. Lumin.* **2021**, *234*, 117937. https://doi.org/10.1016/j.jlumin.2021.117937.
(9) Oh, J.-T.; Lee, S.-Y.; Moon, Y.-T.; Moon, J. H.; Park, S.; Hong, K. Y.; Song, K. Y.; Oh, C.; Shim, J.-I.; Jeong, H.-H.; Song, J.-O.; Amano, H.; Seong, T.-Y. Light Output Performance of Red AlGaInP-Based Light Emitting Diodes with Different Chip Geometries and Structures. *Opt. Express* **2018**, *26* (9), 11194. https://doi.org/10.1364/OE.26.011194.
(10) Tao, Y. B.; Wang, S. Y.; Chen, Z. Z.; Gong, Z.; Xie, E. Y.; Chen, Y. J.; Zhang, Y. F.; McKendry, J.; Massoubre, D.; Gu, E. D.; Rae, B. R.; Henderson, R. K.; Zhang, G. Y. Size Effect on Efficiency Droop of Blue Light Emitting Diode. *Phys. Status Solidi C* **2012**, *9* (3–4), 616–619. https://doi.org/10.1002/pssc.201100483.
(11) Olivier, F.; Tirano, S.; Dupré, L.; Aventurier, B.; Largeron, C.; Templier, F. Influence of Size-Reduction on the Performances of GaN-Based Micro-LEDs for Display Application. *J. Lumin.* **2017**, *191*, 112–116. https://doi.org/10.1016/j.jlumin.2016.09.052.
(12) Daami, A.; Olivier, F.; Dupré, L.; Henry, F.; Templier, F. 59-4: Invited Paper: Electro-Optical Size-Dependence Investigation in GaN Micro-LED Devices. *SID Symp. Dig. Tech. Pap.* **2018**, *49* (1), 790–793. https://doi.org/10.1002/sdtp.12325.
(13) Wong, M. S.; Lee, C.; Myers, D. J.; Hwang, D.; Kearns, J. A.; Li, T.; Speck, J. S.; Nakamura, S.; DenBaars, S. P. Size-Independent Peak Efficiency of III-Nitride Micro-Light-Emitting-Diodes Using Chemical Treatment and Sidewall Passivation. *Appl. Phys. Express* **2019**, *12* (9), 097004. https://doi.org/10.7567/1882-0786/ab3949.
(14) Zhmakin, A. I. Enhancement of Light Extraction from Light Emitting Diodes. *Phys. Rep.* **2011**, *498* (4), 189–241. https://doi.org/10.1016/j.physrep.2010.11.001.
(15) Ley, R. T.; Smith, J. M.; Wong, M. S.; Margalith, T.; Nakamura, S.; DenBaars, S. P.; Gordon, M. J. Revealing the Importance of Light Extraction Efficiency in InGaN/GaN MicroLEDs via Chemical Treatment and Dielectric Passivation. *Appl. Phys. Lett.* **2020**, *116* (25), 251104. https://doi.org/10.1063/5.0011651.
(16) Mei, Y.; Xie, M.; Yang, T.; Hou, X.; Ou, W.; Long, H.; Ying, L.; Liu, Y.; Weng, G.; Chen, S.; Zhang, B. Improvement of the Emission Intensity of GaN-Based Micro-Light Emitting

Diodes by a Suspended Structure. *ACS Photonics* **2022**, *9* (12), 3967–3973. https://doi.org/10.1021/acsphotonics.2c01366.
(17) Zhu, Z.; Tao, T.; Liu, B.; Zhi, T.; Chen, Y.; Yu, J.; Jiang, D.; Xu, F.; Sang, Y.; Yan, Y.; Xie, Z.; Zhang, R. Improved Optical and Electrical Characteristics of GaN-Based Micro-LEDs by Optimized Sidewall Passivation. *Micromachines* **2022**, *14* (1), 10. https://doi.org/10.3390/mi14010010.
(18) Yu, J.; Tao, T.; Liu, B.; Xu, F.; Zheng, Y.; Wang, X.; Sang, Y.; Yan, Y.; Xie, Z.; Liang, S.; Chen, D.; Chen, P.; Xiu, X.; Zheng, Y.; Zhang, R. Investigations of Sidewall Passivation Technology on the Optical Performance for Smaller Size GaN-Based Micro-LEDs. *Crystals* **2021**, *11* (4), 403. https://doi.org/10.3390/cryst11040403.
(19) Park, J.; Baek, W.; Geum, D.-M.; Kim, S. Understanding the Sidewall Passivation Effects in AlGaInP/GaInP Micro-LED. *Nanoscale Res. Lett.* **2022**, *17* (1), 29. https://doi.org/10.1186/s11671-022-03669-5.
(20) Park, J.-H.; Pristovsek, M.; Cai, W.; Cheong, H.; Kumabe, T.; Lee, D.-S.; Seong, T.-Y.; Amano, H. Interplay of Sidewall Damage and Light Extraction Efficiency of Micro-LEDs. *Opt. Lett.* **2022**, *47* (9), 2250–2253. https://doi.org/10.1364/OL.456993.
(21) Shaari, A.; Ahmad Noorden, A. F.; Mohamad, S. N.; Daud, S. GEOMETRICAL ANALYSIS OF LIGHT-EMITTING DIODE FOR ENHANCING EXTRACTION EFFICIENCY. *J. Sustain. Sci. Manag.* **2020**, *15* (6), 68–84. https://doi.org/10.46754/jbsd.2020.08.006.
(22) Djavid, M.; Liu, X.; Mi, Z. Improvement of the Light Extraction Efficiency of GaN-Based LEDs Using Rolled-up Nanotube Arrays. *Opt. Express* **2014**, *22* (S7), A1680. https://doi.org/10.1364/OE.22.0A1680.
(23) Ee, Y.-K.; Kumnorkaew, P.; Arif, R. A.; Tong, H.; Zhao, H.; Gilchrist, J. F.; Tansu, N. Optimization of Light Extraction Efficiency of III-Nitride LEDs With Self-Assembled Colloidal-Based Microlenses. *IEEE J. Sel. Top. Quantum Electron.* **2009**, *15* (4), 1218–1225. https://doi.org/10.1109/JSTQE.2009.2015580.
(24) Ryu, H.-Y.; Pyo, J.; Ryu, H. Y. Light Extraction Efficiency of GaN-Based Micro-Scale Light-Emitting Diodes Investigated Using Finite-Difference Time-Domain Simulation. *IEEE Photonics J.* **2020**, *12* (2), 1–10. https://doi.org/10.1109/JPHOT.2020.2977401.
(25) Drouin, D.; Couture, A. R.; Joly, D.; Tastet, X.; Aimez, V.; Gauvin, R. CASINO V2.42—A Fast and Easy-to-Use Modeling Tool for Scanning Electron Microscopy and Microanalysis Users. *Scanning* **2007**, *29* (3), 92–101. https://doi.org/10.1002/sca.20000.
(26) Li, K. H.; Cheung, Y. F.; Tang, C. W.; Zhao, C.; Lau, K. M.; Choi, H. W. Optical Crosstalk Analysis of Micro-Pixelated GaN-Based Light-Emitting Diodes on Sapphire and Si Substrates. *Phys. Status Solidi A* **2016**, *213* (5), 1193–1198. https://doi.org/10.1002/pssa.201532789.
(27) Olivier, F.; Daami, A.; Licitra, C.; Templier, F. Shockley-Read-Hall and Auger Non-Radiative Recombination in GaN Based LEDs: A Size Effect Study. *Appl. Phys. Lett.* **2017**, *111* (2), 022104. https://doi.org/10.1063/1.4993741.
(28) Hafiz, S.; Zhang, F.; Monavarian, M.; Avrutin, V.; Morkoç, H.; Özgür, Ü.; Metzner, S.; Bertram, F.; Christen, J.; Gil, B. Determination of Carrier Diffusion Length in GaN. *J. Appl. Phys.* **2015**, *117* (1), 013106. https://doi.org/10.1063/1.4905506.
(29) Kumakura, K.; Makimoto, T.; Kobayashi, N.; Hashizume, T.; Fukui, T.; Hasegawa, H. Minority Carrier Diffusion Length in GaN: Dislocation Density and Doping Concentration Dependence. *Appl. Phys. Lett.* **2005**, *86* (5), 052105. https://doi.org/10.1063/1.1861116.

(30) Yakimov, E. B. Diffusion Length Measurements in GaN. *Jpn. J. Appl. Phys.* **2016**, *55* (5S), 05FH04. https://doi.org/10.7567/JJAP.55.05FH04.
(31) Kumakura, K.; Makimoto, T.; Kobayashi, N.; Hashizume, T.; Fukui, T.; Hasegawa, H. Minority Carrier Diffusion Lengths in MOVPE-Grown n- and p-InGaN and Performance of AlGaN/InGaN/GaN Double Heterojunction Bipolar Transistors. *J. Cryst. Growth* **2007**, *298*, 787–790. https://doi.org/10.1016/j.jcrysgro.2006.10.098.
(32) David, A. Long-Range Carrier Diffusion in (In,Ga)N Quantum Wells and Implications from Fundamentals to Devices. *Phys. Rev. Appl.* **2021**, *15* (5), 054015. https://doi.org/10.1103/PhysRevApplied.15.054015.
(33) Cremades, A.; Albrecht, M.; Voigt, A.; Krinke, J.; Dimitrov, R.; Ambacher, O.; Stutzmann, M. Minority Carrier Diffusion Length in AlGaN: A Combined Electron Beam Induced Current and Transmission Microscopy Study. *Solid State Phenom.* **1998**, *63–64*, 139–146. https://doi.org/10.4028/www.scientific.net/SSP.63-64.139.
(34) Olivier, F.; Daami, A.; Dupré, L.; Henry, F.; Aventurier, B.; Templier, F. 25-4: Investigation and Improvement of 10μm Pixel-Pitch GaN-Based Micro-LED Arrays with Very High Brightness. *SID Symp. Dig. Tech. Pap.* **2017**, *48* (1), 353–356. https://doi.org/10.1002/sdtp.11615.
(35) Pozina, G.; Ciechonski, R.; Bi, Z.; Samuelson, L.; Monemar, B. Dislocation Related Droop in InGaN/GaN Light Emitting Diodes Investigated via Cathodoluminescence. *Appl. Phys. Lett.* **2015**, *107* (25), 251106. https://doi.org/10.1063/1.4938208.
(36) Doan, M.-H.; Lee, J. Spatially Resolved Cathodoluminescence in the Vicinity of Defects in the High-Efficiency InGaN/GaN Blue Light Emitting Diodes. *Adv. Condens. Matter Phys.* **2014**, *2014*, 1–5. https://doi.org/10.1155/2014/671210.
(37) Weatherley, T. F. K.; Liu, W.; Osokin, V.; Alexander, D. T. L.; Taylor, R. A.; Carlin, J.-F.; Butté, R.; Grandjean, N. Imaging Nonradiative Point Defects Buried in Quantum Wells Using Cathodoluminescence. *Nano Lett.* **2021**, *21* (12), 5217–5224. https://doi.org/10.1021/acs.nanolett.1c01295.
(38) Liu, Y.; Feng, F.; Zhang, K.; Jiang, F.; Chan, K.-W.; Kwok, H.-S.; Liu, Z. Analysis of Size Dependence and the Behavior under Ultrahigh Current Density Injection Condition of GaN-Based Micro-LEDs with Pixel Size down to 3 Mm. *J. Phys. Appl. Phys.* **2022**, *55* (31), 315107. https://doi.org/10.1088/1361-6463/ac6cb4.
(39) Hangleiter, A.; Langer, T.; Henning, P.; Ketzer, F. A.; Bremers, H.; Rossow, U. Internal Quantum Efficiency of Nitride Light Emitters: A Critical Perspective. In *Gallium Nitride Materials and Devices XIII*; SPIE, 2018; Vol. 10532, pp 132–139. https://doi.org/10.1117/12.2290082.
(40) Lähnemann, J.; Kaganer, V. M.; Sabelfeld, K. K.; Kireeva, A. E.; Jahn, U.; Chèze, C.; Calarco, R.; Brandt, O. Carrier Diffusion in GaN -- a Cathodoluminescence Study. III: Nature of Nonradiative Recombination at Threading Dislocations. *Phys. Rev. Appl.* **2022**, *17* (2), 024019. https://doi.org/10.1103/PhysRevApplied.17.024019.
(41) Wolter, S.; Spende, H.; Gülink, J.; Hartmann, J.; Wehmann, H.-H.; Waag, A.; Lex, A.; Avramescu, A.; Lugauer, H.-J.; von Malm, N.; Drolet, J.-J.; Strassburg, M. Size-Dependent Electroluminescence and Current-Voltage Measurements of Blue InGaN/GaN MLEDs down to the Submicron Scale. *Nanomaterials* **2021**, *11* (4), 836. https://doi.org/10.3390/nano11040836.

**TOC**